JOURNAL OF MATERIALS SCIENCE 21 (1986) 2365–2372

Effect of test method and crack size on the fracture toughness of a chain-silicate glass–ceramic

G. H. BEALL, K. CHYUNG, R. L. STEWART
Corning Glass Works, Corning, New York 14831, USA

K. Y. DONALDSON, H. L. LEE, S. BASKARAN, D. P. H. HASSELMAN
Department of Materials Engineering, Virginia Polytechnic Institute and State University, Blacksburg, Virginia 24061, USA

The fracture toughness of a canasite glass–ceramic with a highly acicular, interlocked grain structure was measured by a number of different methods. The values at room temperature obtained by the chevron-notch, short-bar and notched-beam methods ranged from 4 to 5 MPa $m^{-1/2}$, well above literature values for other glass–ceramics. Similar values of toughness were obtained by the fracture of bars with indentation cracks introduced with loads ranging from 1.96 to 400 N, but only for crack sizes $>200\,\mu m$, with lower values for cracks of smaller size. The toughness values obtained by the direct measurement of the size of the indentation cracks were appreciably lower than the values obtained by all other methods over the total range of indentation loads and corresponding crack size. SEM fractography showed that the surface within the indentation cracks was appreciably smoother than the surrounding fracture surface. The high values of fracture toughness were attributed to the combined mechanisms of crack-deflection and microcrack-toughening due to the stress-enhanced creation of microcracks caused by the residual stresses which arise from the thermal expansion anisotropy of the canasite monoclonic crystal structure. The strong negative temperature dependence of the fracture toughness suggests that at room temperature microcrack toughening represents the primary contributing mechanism to the fracture toughness. The combined effects of crack-deflection and microcrack-toughening can lead to the development of glass–ceramics with greatly improved resistance to crack propagation.

1. Introduction

Structural ceramics, because of their high resistance to corrosion and deformation by creep, as well as their excellent resistance to chemical and abrasive wear, are eminently suited for engineering applications involving severe operating conditions and elevated temperatures. Unfortunately, the successful use of structural ceramics is handicapped by their high degree of brittleness, which results in low strains-to-fracture, low resistance to mechanical surface damage, low resistance to impact and high susceptibility to catastrophic failure under conditions of thermal shock [1]. However, significant improvements in these latter unfavourable properties of brittle ceramics can be achieved by increasing the resistance to crack propagation (i.e., the fracture toughness).

Toughening of brittle materials can be accomplished in a variety of ways. The presence of a ductile metallic grain-boundary phase, as exemplified by cobalt-bonded tungsten carbide, is a highly effective toughening agent. Other mechanisms of toughening, recognized as effective in increasing the fracture toughness of structural ceramics as well as of other brittle solids, include transformation toughening by means of a dispersed phase of tetragonal zirconia [2, 3], stress-induced microcracking [4, 5], and crack-deflection by tilt or twist around a second phase inclusion [6]. For fibre (or whisker) reinforced brittle materials, toughening mechanisms include fibre fracture and pull-out and/or ligament toughening due to fibres which bridge the crack opening at locations behind the crack front [7].

Crack deflection as a toughening mechanism can occur in polycrystalline brittle materials with preferred crystallographic cleavage planes. The development of a columnar grain structure with preferred orientation was found to improve the fracture toughness of silicon nitride [8]. Toughening by crack deflection can also be promoted by the presence of a high toughness second phase around which the crack in the matrix must propagate [6, 9].

Glass–ceramic materials can also be toughened by control over the microstructure which results from the crystallization process. The superior fracture toughness of a series of cordierite glass–ceramics was attributed to the deflection of the propagating crack around the larger crystallites of higher fracture toughness embedded in a fine-grained matrix of lower

0022–2461/86 $03.00 + .12

fracture toughness [10]. In comparison to glass–ceramics with a more equidimensional grain shape, glass–ceramic materials with highly acicular crystal structures whould exhibit superior fracture toughness as the result of enhanced crack deflection. In particular, acicular microstructures are found in chain-silicate glass–ceramics in which, because of a preferred growth direction, crystallization results in a highly interlocked acicular grain structure. The purpose of this study was to investigate the fracture toughness of such a chain-silicate glass–ceramic.

2. Experimental details

2.1. Material

The specific chain-silicate glass–ceramic selected for this study is based on the mineral canasite with composition corresponding to $Ca_5Na_4K_2Si_{12}O_{30}F_4$ which exists in the monoclinic crystal structure with easy cleavage fracture occurring along the (1 0 0) and (0 0 1) planes. The lattice parameters a, b and c at room temperature were 1.8844, 0.7283 and 1.2693 nm, respectively, with corresponding coefficients of thermal expansion of 10.525×10^{-6}, 9.263×10^{-6} and $16.000 \times 10^{-6\circ}C^{-1}$ determined from X-ray data obtained from 25 to 700° C. The angle β at room temperature equalled 112.27° with a coefficient of thermal expansion of $-4.48 \times 10^{-6\circ}C^{-1}$. The samples were made from the original glass with CaF_2 as nucleating agent by a nucleation stage at 560° C for 4 h followed by crystal growth at 880° C for 4 h for measurement of the fracture toughness by the indentation method, and for 4 or 49 h for toughness measurement by the other methods. The glass–ceramic samples made in this manner were approximately 90% crystalline with the remainder consisting of the primarily glassy phase. Young's modulus and Poisson's ratio at room temperature were measured to be 85.5 GPa and 0.22, respectively. Details of the microstructure will be presented subsequently in the form of SEM fractographs to illustrate the data for fracture toughness.

2.2. Measurement of fracture toughness

The fracture toughness K_{Ic}, at room temperature, was measured by five different methods:

1. The indentation-fracture method was used with a Vickers indenter as described by Evans and Charles [11], which relies on the direct measurement of the size of the indentation cracks along a polished surface, which for the present samples was annealed at 600° C for 4 h to reduce or eliminate residual stresses introduced by the polishing. Indentation loads ranged from 1.96 N up to 500 N. A conventional microhardness tester was used for indentation loads < 20 N. For loads > 20 N, a servo-electric mechanical tester was programmed to apply the load in a load–time sequence identical to the one for the microhardness tester. From the data of crack size and the dimensions of the indent diagonal, the fracture toughness K_{Ic} at any given load was calculated by means of the expression of Niihara *et al.* [12] for indentation cracks with the median crack geometry.

2. The indentation-strength method, which relies on the measurement of the load required to fracture an indented specimen, is described by Chantikul *et al.* [13]. The specimens for this purpose consisted of bars measuring approximately 5 mm × 2.5 mm × 65 mm and were cut from a larger block with a low speed diamond saw. The specimens were indented in the centre of one of the 5 × 65 mm faces. The indentation loads ranged from 1.96 to 400 N, and were applied using the microhardness tester for loads < 20 N and a servo-hydraulic tester for loads > 20 N, as described earlier. In order to minimize sub-critical crack growth over the time period between indentation and the fracture test, a drop of immersion oil was placed on the site of the indentation prior to the indentation process. With the indentation on the tensile surface, the specimens were broken in four-point bending using an inner and outer span of 25 and 38 mm, respectively, at a stressing rate of ~ 10 MPa sec^{-1}. From the indentation load and load at failure the fracture toughness was calculated with the aid of the expression given by Chantikul *et al.* [13].

3. The single-edge notched-beam (SENB) method was used, as described by Brown and Srawley [14], using rectangular bar specimens with dimensions of ~ 5 mm × 5 mm × 45 mm. A transverse saw cut with depth ~ 2.5 mm was introduced with a diamond blade of thickness ~ 0.17 mm. The notched bars were broken in four-point bending with inner and outer spans of 20 and 40 mm, respectively, at a cross-head speed of 0.017 mm sec^{-1}. The fracture toughness was calculated from the dimensions of the bar, the inner and outer spans and the magnitude of the failure load by means of the expression given by Brown and Srawley [14].

4. The Chevron-notch method was used as described by Munz *et al.* [15]. Specimens measured approximately 5 mm × 6 mm × 45 mm, with the Chevron notch cut with the aid of a diamond blade with a width of ~ 0.17 mm to a depth of ~ 4.5 mm along the sides of the specimen, and the depth of the tip of the Chevron from the tensile surface ranging from 0.1 to 0.4 mm. The specimens were fractured in an Instron tester in four-point bending with inner and outer spans of 12.5 and 40 mm, respectively, at a cross-head speed of 8.3×10^{-4} mm sec^{-1}. The fracture toughness was calculated with the aid of the expression given by Munz *et al.* [15] from the dimensions of the specimens and the notch and the maximum load.

5. The short-bar method was used, as described by Munz *et al.* [16], using specimens with cross-section of 9.6 mm × 8.4 mm by 14.3 mm long, and a notch-depth of ~ 1.6 mm at the front of the notch and ~ 10 mm along the side of the specimen which yields a notch angle of $\sim 58°$. The notch was cut with a diamond-saw blade with thickness of ~ 0.17 mm. The fracture toughness was calculated by means of the relation given by Munz *et al.* [16] from the maximum value of load encountered during fracture and the dimensions of the specimen and notch.

The Chevron-notch method was also used for the

measurement of fracture toughness as a function of temperature.

SEM-fractography was used to obtain information on the morphology of the fracture surface and on the mechanisms of toughening.

3. Results, discussion and conclusions

Table I lists the mean values for the fracture toughness at room temperature for the canasite glass–ceramics crystallized for 4 and 49 h at 880° C, measured by the single-edge notched-beam, the chevron-notch and the short-bar methods. The differences in values for the three test methods cannot be judged to be significantly different. The crystallization treatment of 49 h appears to yield a somewhat higher value for the toughness than the crystallization of 4 h. It is encouraging to note that regardless of the test method or duration of crystallization, the data for the fracture toughness of this chain-silicate glass–ceramic are about 2 to 4 times the corresponding values typical for non-chain-silicate glass–ceramics [12, 17, 18].

Fig. 1 shows the dependence of fracture toughness on temperature of the canasite glass–ceramic crystallized for 49 h measured by the chevron-notch method. Over the range from 25 to 600° C, the toughness decreases rather rapidly by a factor of almost five. This large negative temperature dependence is much larger than the corresponding temperature dependence observed for many other brittle materials [19, 20, 21]. The value of $K_{Ic} \sim 1$ at 600° C is of the order expected for brittle materials undergoing pure mode I crack propagation in the absence of any additional toughening mechanisms.

Figs 2a, b, c, d and e show SEM fractographs of the chevron-notch specimens used for the acquisition of the data presented in Fig. 1 at 25, 200, 400, 600 and 800° C, respectively. The acicular interlocked crystal structure is clearly evident from the fracture surface created at 25° C and shown in Fig. 2a. This fracture surface also indicates significant out-of-plane crack propagation as the result of a high degree of crack deflection. As indicated by Figs 2a, b, c and d, the fracture surfaces become increasingly smoother with increasing temperature up to about 600° C, indicating a decrease in the degree of non-planar crack propagation. It should be noted that this decrease in surface roughness with increasing temperature correlates with a corresponding decrease in fracture toughness.

At 800° C, as indicated by the fracture surface shown in Fig. 2e, crack propagation appears to be accompanied by viscous flow of the residual glassy phase, which appears to have spread over nearly the total fracture surface. The viscous flow of this glassy phase is thought to be responsible for the increase in fracture toughness from 600 to 800° C, as shown in Fig. 1.

TABLE I Fracture toughness at room temperature of chain-silicate canasite glass–ceramic crystallized for 4 or 49 h measured by three different methods

Method	Fracture toughness ($MN\,m^{-3/2}$)	
	4 h*	49 h*
Single-edge notched-beam	4.48 ± 0.31†(10)‡	5.11 ± 0.22†(10)‡
Chevron-notch	4.41 ± 0.30(5)	4.78 ± 0.34(5)
Short-bar	4.12 ± 0.31(3)	4.88 ± 0.27(3)

*Period of crystallization at 880° C following nucleation at 560° C for 4 h.
†Standard deviation.
‡Number of data points.

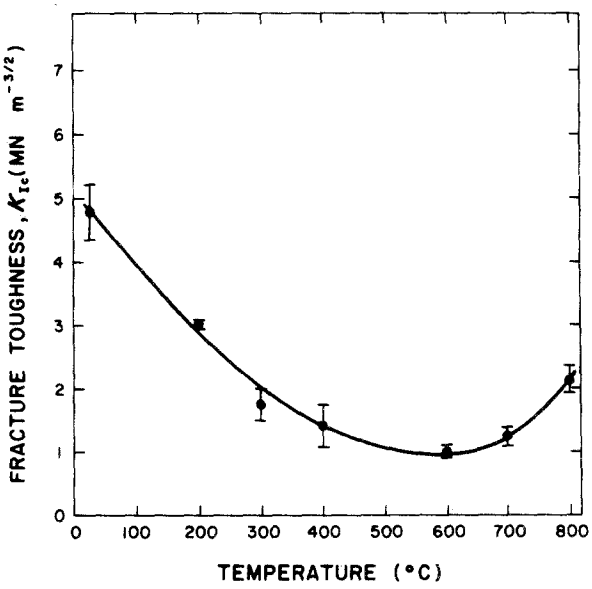

Figure 1 Temperature dependence of the fracture toughness of canasite glass–ceramic crystallized for 40 h measured by the chevron-notch method.

Figs 3a, b and c show the data for the half-diagonal, the crack size and the calculated data for the fracture toughness as a function of indentation load determined by the direct measurement of the crack size, respectively, for the canasite glass–ceramic crystallized for 4 h. The data for the half-diagonal and crack size are continuous over the total range of indentation load. This suggests that the technique of loading (hardness tester as opposed to servo-hydraulic tester) does not affect the results obtained. The value of the slope of the data for the size of the half-diagonal as a function of indentation load has a value very close to 1/2, which is the value expected for a hardness which is independent of load. However, the slope of the data for the crack size as a function of indentation load has a value near 0.6, which is somewhat below the value of 2/3 expected for median indentation cracks in a brittle near 0.6, which is somewhat below the value of 2/3 expected for median indentation cracks in a brittle solid with crack-size independent fracture toughness [22]. This lower value of slope suggests that the fracture toughness increases with increasing crack size, supported by the trend of the data for fracture toughness as a function of indentation load shown in Fig. 3c. This behaviour is indicative of a toughening mechanism with an effectiveness which increases with crack size.

For purposes of comparison, Fig. 3c also shows the value of fracture toughness obtained by the single-edge notched-beam technique. It is clearly evident that the values obtained by the indentation-fracture method are significantly lower than those obtained by the SENB technique over the total range of indentation load.

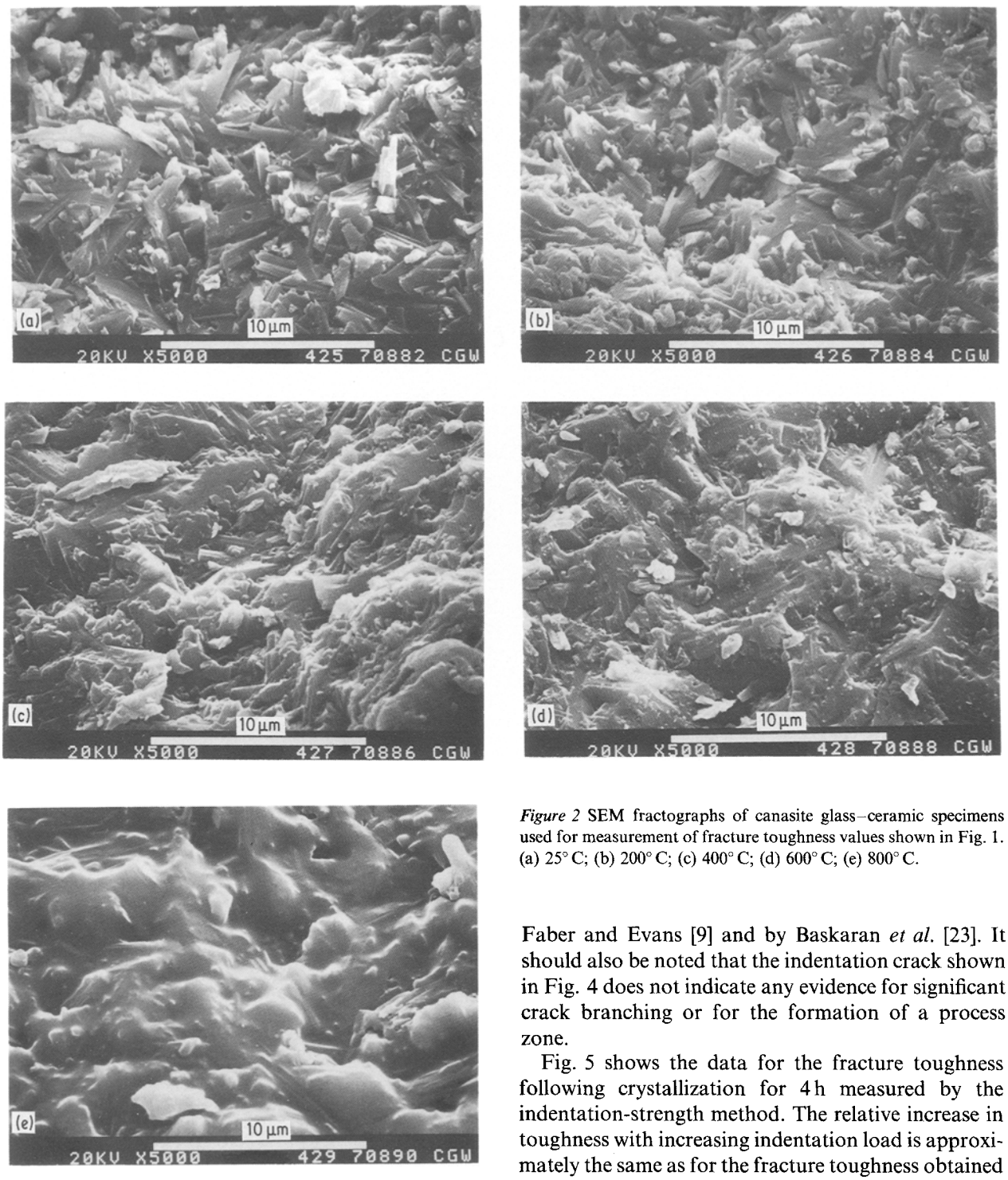

Figure 2 SEM fractographs of canasite glass–ceramic specimens used for measurement of fracture toughness values shown in Fig. 1. (a) 25° C; (b) 200° C; (c) 400° C; (d) 600° C; (e) 800° C.

Fig. 4 shows a typical indentation crack in a surface of the canasite glass–ceramic which was given a light HF etch to bring out the microstructural details. The non-planar mode of propagation of the crack suggests that crack-deflection is a possible contributing mechanism to the fracture toughness. However, the degree of out-of-plane propagation of the surface crack shown in Fig. 4 appears to be much less than the degree expected from the acicular nature of the microstructure clearly evident in Fig. 2, if crack propagation takes place around the crystallites. This suggests that fracture takes place through the crystallites, a mechanism which tends to diminish the full benefit that can be obtained from crack deflection as a toughening mechanism. This phenomenon was also observed by Faber and Evans [9] and by Baskaran *et al.* [23]. It should also be noted that the indentation crack shown in Fig. 4 does not indicate any evidence for significant crack branching or for the formation of a process zone.

Fig. 5 shows the data for the fracture toughness following crystallization for 4 h measured by the indentation-strength method. The relative increase in toughness with increasing indentation load is approximately the same as for the fracture toughness obtained by the indentation-fracture method, shown in Fig. 3c. However it is significant that over the total range of indentation load the fracture toughness obtained by the strength method exceeds the value obtained by the indentation-fracture method by more than a factor of two. It is also noteworthy that for indentation loads in excess of about 20 N, the fracture toughness obtained from the indentation-strength method agrees very well with the value of fracture toughness obtained by the SENB and other methods listed in Table I.

Figs 6a and b show SEM fractographs of the surface of a strength specimen with an indentation crack introduced at a load of 5 N, inside and outside the area of the original indentation crack, respectively. Comparison of these fracture surfaces indicates that the surface of the original indentation crack is much smoother than the fracture surface surface outside the indentation

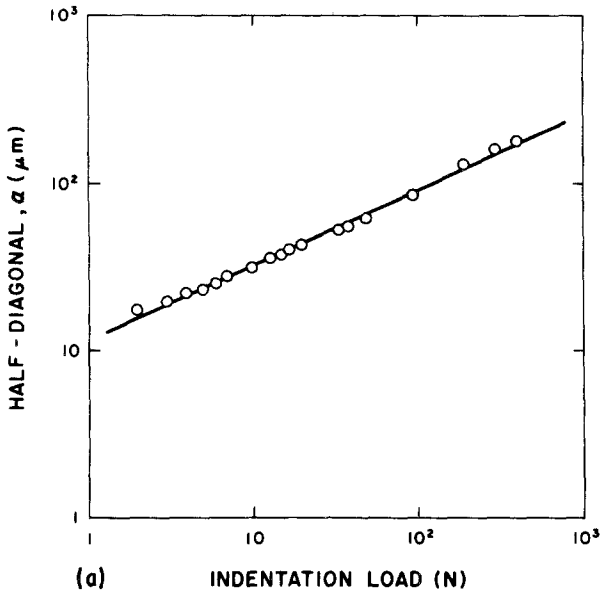

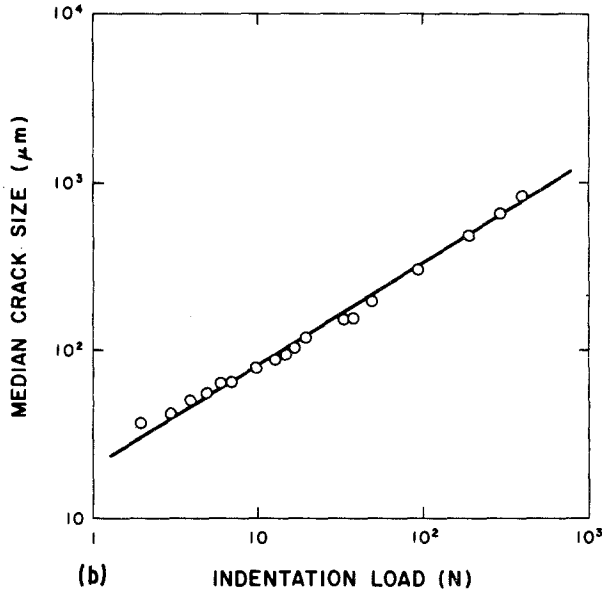

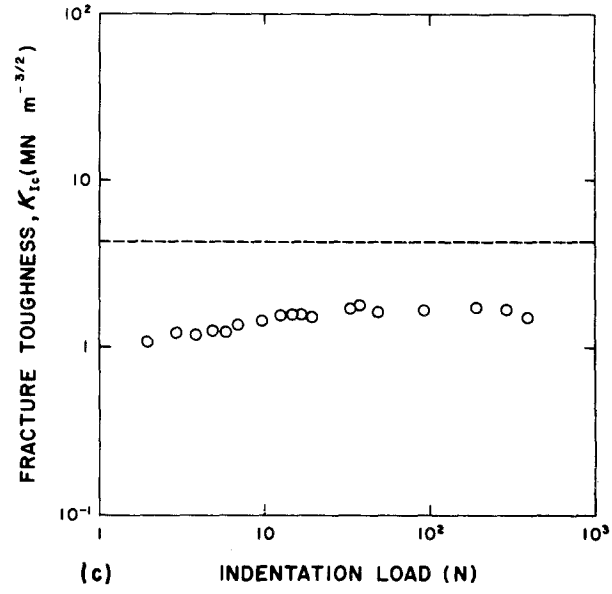

Figure 3 Indentation fracture data for canasite glass–ceramic crystallized for 4 h. (a) Half-diagonal; (b) medium crack size; and (c) fracture toughness calculated from measured crack size. (○) Measurement of crack size; (– – –) single edge notched beam.

crack. Similar differences are shown by the corresponding fracture surfaces for a strength specimen indented with a load of 161 N shown in Fig. 7. It is suggested that these differences in surface morphology provide an explanation for the differences in the values of the fracture toughness obtained by the indentation-fracture method and strength method given in Figs 3c and 5.

By combining the data shown in Figs 3, 4 and 5, the fracture toughness can be plotted directly as a function of indentation crack size, as shown in Fig. 8. These data indicate that a minimum crack size of $\sim 200\,\mu$m is required for the fracture toughness obtained by the strength method to be equal to the toughness value obtained by the SENB and the other two methods listed in Table I. For crack sizes $< 200\,\mu$m, the fracture toughness decreases rapidly with decreasing crack size.

In summary, the principal observations of the fracture behaviour of the canasite chain-silicate glass–ceramic of this study include:

1. The fracture toughness obtained by the indentation-fracture method is less than the corresponding

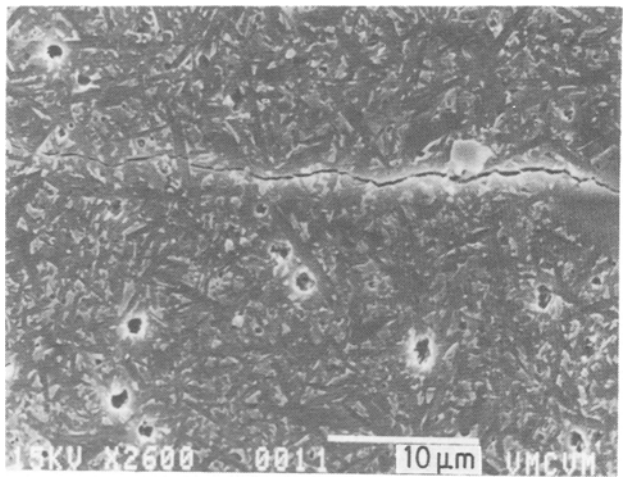

Figure 4 Indentation crack in canasite glass–ceramic crystallized for 4 h introduced at load of 9.8 N.

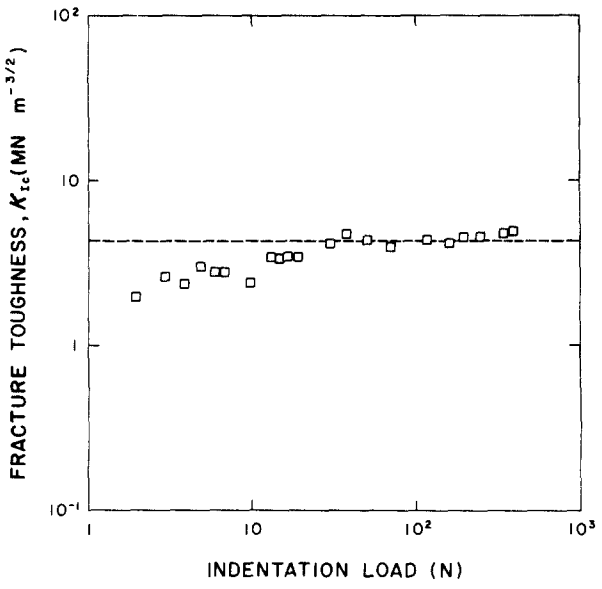

Figure 5 Fracture toughness of canasite glass–ceramics crystallized for 4 h measured by indentation-strength method at room temperature. (□) Strength method; (– – –) single edge notched beam.

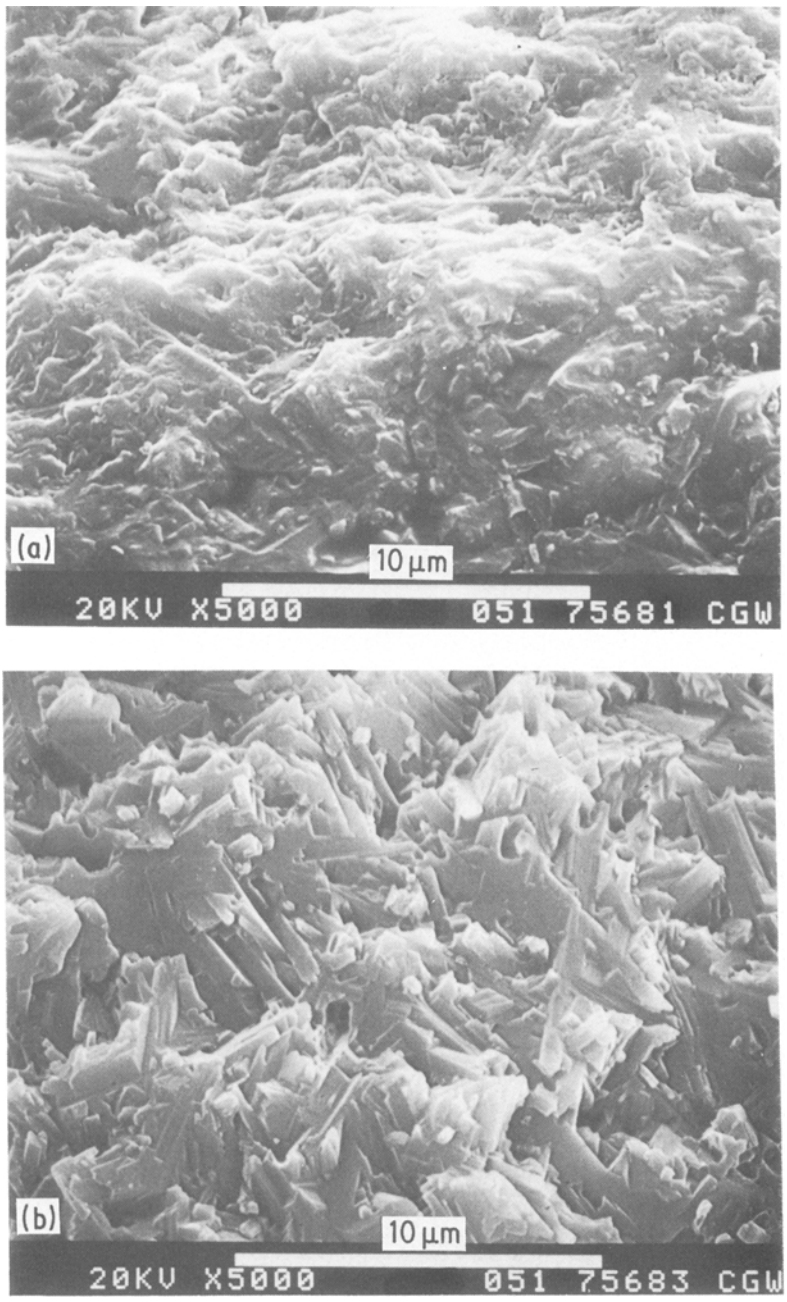

Figure 6 SEM-fractographs of indentation strength specimen used for the fracture toughness data shown in Fig. 5 at indentation load of 5 N, (a) inside original indentation; (b) outside indentation.

values obtained by the indentation-strength method for the same values of indentation load.

2. The fracture toughness obtained by both indentation-fracture and indentation-strength methods shows significant increases with crack length. For indentation cracks > 200 μm, the data obtained by the indentation-strength method agree with the values of fracture toughness obtained by the single-edge notched-beam, the chevron-notch, and the short-bar methods.

3. The fracture toughness measured by the chevron-notch method shows a strong negative temperature dependence, which correlates with a corresponding decrease in the roughness of the fracture surface.

The above observations must be explained in terms of the primary mechanisms of toughening and the effect of the test method on the measured value of fracture toughness. The following hypotheses are subject to verification by future theoretical analysis.

The fracture toughness of the chain-silicate glass–ceramic appears to be affected by two primary mechanisms: (1) crack-deflection, which arises from the combined effects of the acicular microstructure and the preferred cleavage fracture, and (2) stress-induced microcrack toughening, due to the internal stresses caused by the anisotropy in thermal expansion of the individual crystals, which leads to microcracking by intergranular or intragranular cleavage fracture. It is suggested that although toughening by crack deflection may play a role at room temperature, microcrack-toughening makes the major contribution to the observed value of fracture toughness. The principal basis for this conclusion is the observed rapid decrease in fracture toughness with increasing temperature shown in Fig. 1. Microcrack toughening results from the internal stresses which arise from the thermal expansion anisotropy of the individual grains. The magnitude of these internal stresses is proportional to the temperature range over which the glass–ceramic is in the elastic state on cooling from the crystallization temperature. For this reason, the stresses are a

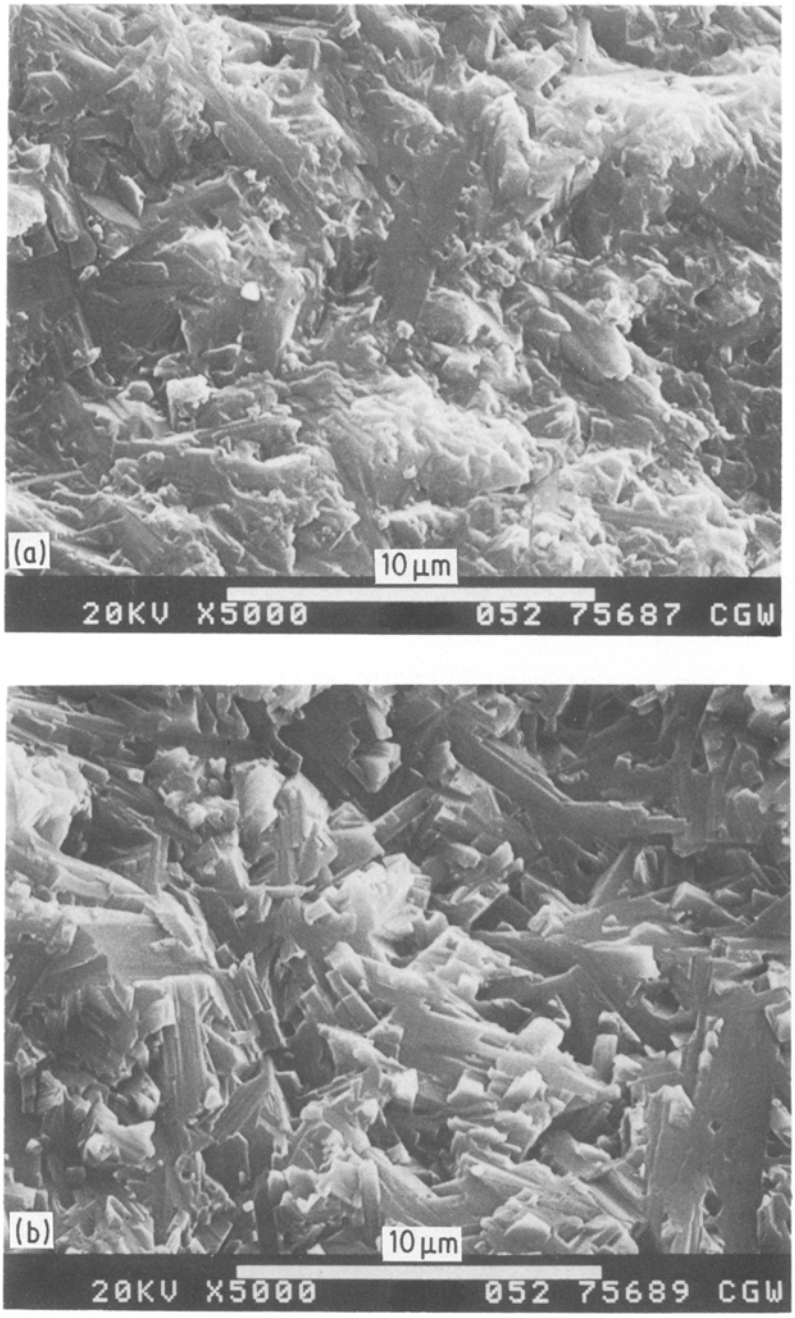

Figure 7 SEM-fractographs of indentation strength specimen used for fracture toughness data shown in Fig. 5 for indentation load of 161 N, (a) inside original indentation; (b) outside indentation.

maximum at room temperature and will decrease in magnitude with increasing temperature. Therefore, for a given microstructure, the incidence of stress-induced microcracking is expected to decrease with increasing temperature, accompanied by an associated decrease in fracture toughness. The evidence for crack-deflection indicated by the fracture surface, shown in Fig. 2a, in the view of these authors, in fact represents evidence for the formation of microcracks by cleavage or grain-boundary fracture within the highly-stressed zone ahead of the crack tip, which then provides a path of preferential propagation for the main crack along the plane of the microcracks. As a result of the decreasing incidence of microcracking with increasing temperature, the fracture surfaces are expected to show a decrease in surface roughness. This is in agreement with the observations shown in Fig. 3 and also indicates that the formation of the fracture surfaces is governed to a considerable extent by fracture through the crystallites rather than by fracture around the crystallites. The existence of fracture through the crystallites is also supported by the fractograph of the indentation shown in Fig. 4. The path of propagation of this crack, as pointed out earlier, indicates a much smaller degree of crack-deflection than expected if crack propagation had occurred around the crystallites. It is recognized that the presence of internal stresses will also promote crack-deflection and thereby increase fracture toughness. This mechanism also should exhibit a strong negative temperature dependence. In view of this, microcrack toughening is thought to be the major contributing mechanism to the high value of fracture toughness at room temperature of the glass–ceramic of this study.

The differences in the data for the fracture toughness obtained by the indentation-fracture method and the indentation-strength method is thought to be due to the differences in the magnitudes and/or distribution of the stress fields in the vicinity of the cracks for these two methods. In order to explain the

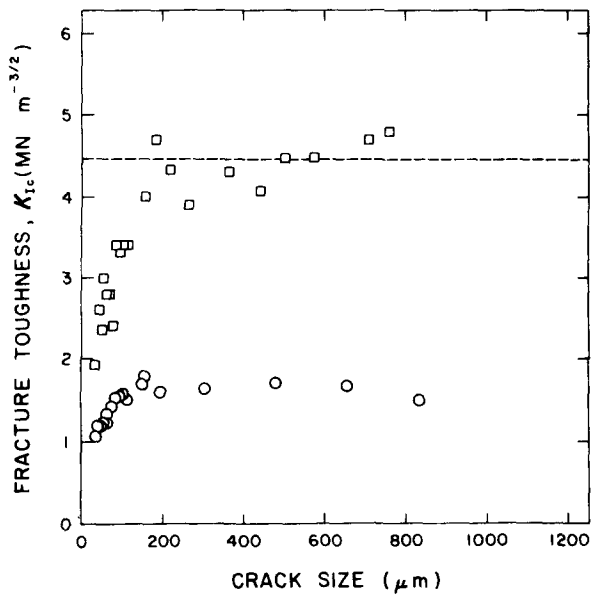

Figure 8 Indentation fracture toughness of canasite glass–ceramic crystallized for 4 h as a function of indentation crack size obtained by strength method and measurement of crack size. (□) Strength method; (○) measurement of crack size; (– – –) single edge notched beam.

dependence of crack size on indentation load, Lawn and Fuller [24] and Evans and Charles [11] pointed out that the loading on a median crack formed under the influence of the residual stress field around the indentation is mechanically equivalent to a penny-shaped crack opened by a force P at its centre. Alternatively, the loading condition on the crack can be represented by a fixed crack-opening displacement at its centre, with crack formation serving as a mechanism for the relief of the residual stresses. In this manner, the final size of the indentation crack corresponds to the condition of crack arrest. It is speculated that under this latter condition the driving force derived from the relaxation of the residual stress field just suffices to supply the energy required to propagate the crack along a single crack front with little or no probability for secondary crack or microcrack formation. Under these conditions, the mechanism of microcrack toughening and associated crack-size dependence will largely be suppressed. A different condition prevails when a mechanical load is applied to an indented specimen. In this situation, the driving force required for crack propagation is supplied continuously by the external stress field, which can provide sufficient energy for microcrack formation, especially as the crack becomes larger at constant load. Under these conditions the mechanism of microcrack toughening will be fully effective. Clearly, the validity of the above hypothesis is subject to future theoretical analysis. But if shown to be valid, it should predict that for any toughening mechanism which relies on a stress-induced process, such a microcrack-toughening or transformation-toughening, the fracture toughness obtained by the indentation-fracture method should be less than the corresponding value obtained by the indentation-strength method at the same value of indentation load, or less than the toughness obtained by any other method which relies on the onset of failure or extended crack propagation.

In conclusion, it appears that as the result of its acicular microstructure, in combination with its monoclinic crystal structure, chain-silicate canasite glass–ceramic exhibits high values of fracture toughness at room temperature attributable to toughening by crack-deflection and stress-induced microcrack formation.

Acknowledgements

Specimen fabrication and the measurement of the fracture toughness by the single-edge notched-beam, the chevron-notch and short-bar methods were performed at Corning Glass Works. The indentation toughness was measured at Virginia Polytechnic Institute as part of a research program funded by the Office of Basic Energy Sciences, Department of Energy, under Contract DE-A505-82-ER-10937.

References

1. D. P. H. HASSELMAN, *J. Amer. Ceram. Soc.* **52** (1969) 600.
2. A. G. EVANS and A. HEUER, *ibid.* **63** (1980) 241.
3. R. M. McMEEKING and A. G. EVANS, *ibid.* **65** (1982) 242.
4. Y. FU and A. G. EVANS, *Acta Metall.* **30** (1982) 1619.
5. A. G. EVANS and K. T. FABER, *J. Amer. Ceram. Soc.* **67** (1984) 255.
6. K. T. FABER and A. G. EVANS, *Acta Metall.* **31** (1983) 565.
7. A. G. EVANS, A. H. HEUER and D. L. PORTER, Proceedings of the Fourth International Conference on Fracture, edited by D. M. R. Taplin (University of Waterloo Press, 1977) Vol. 1, p. 529.
8. F. F. LANGE, *J. Amer. Ceram. Soc.* **56** (1973) 518.
9. K. T. FABER and A. G. EVANS, *Acta Metall.* **31** (1983) 577.
10. R. MORENA, K. NIIHARA and D. P. H. HASSELMAN, *J. Amer. Ceram. Soc.* **66** (1983) 673.
11. A. G. EVANS and E. A. CHARLES, *ibid.* **59** (1976) 371.
12. K. NIIHARA, R. MORENA and D. P. H. HASSELMAN, *J. Mater. Sci. Lett.* **1** (1982) 13.
13. P. CHANTIKUL, G. R. ANSTIS, B. R. LAWN and D. B. MARSHALL, *J. Amer. Ceram. Soc.* **64** (1981) 539.
14. W. F. BROWN Jr and J. E. SRAWLEY, ASTM Special Technical Publication 410 (American Society for Testing and Materials, Philadelphia, Pennsylvania, 1966) 13.
15. D. G. MUNZ, J. L. SHANNON and R. T. BUBSEY, *Int. J. Fracture* **16** (1980) R137.
16. D. G. MUNZ, R. T. BUBSEY and J. E. SRAWLEY, *ibid.* **16** (1980) 359.
17. J. C. SWEARENGEN and R. J. EAGAN, *J. Mater. Sci.* **11** (1976) 1857.
18. B. G. KOEPKE, K. D. McHENRY and W. D. SAVAGE, *Bull. Amer. Ceram. Soc.* **58** (1979) 1100.
19. R. C. BRANDT, D. P. H. HASSELMAN and F. F. LANGE, (eds), "Fracture mechanics of Ceramics", Vols. 1 and 2 (Plenum Press, New York, 1974).
20. *Idem*, Vols. 3 and 4 (Plenum, New York, 1978).
21. *Idem*, Vols. 5 and 6 (Plenum, New York, 1983).
22. B. R. LAWN, in "Fracture Mechanics of Ceramics", Vol. 5, edited by R. C. Bradt, A. G. Evans, D. P. H. Hasselman and F. F. Lange (Plenum Press, New York, 1983) p. 1.
23. S. BASKARAN, S. B. BHADURI and D. P. H. HASSELMAN, *J. Amer. Ceram. Soc.* **68** (1985) 112.
24. B. R. LAWN and E. R. FULLER, *J. Mater. Sci.* **10** (1975) 2016.

Received 16 July
and accepted 13 September 1985